PHYSICAL SCIENCE OF MATERIALS

UDC 53.06
EDN: UIVSCB
PACS: 87.50.wp, 78.70.Ps

Optical properties of calcium tungstate doped with various lanthanides (Pr, Nd, Eu, Ce, Sm)

© P. D. Kuznetsova*, E. A. Mukhanova, K. K. Volik, I. A. Pankin, A.V. Soldatov

International Research Institute of Smart Materials of the Southern Federal University, Rostov-on-Don, 344090 Russia
** E-mail: pkuznecova@sfedu.ru*

Received 29.09.2024; revised 09.01.2025; accepted 07.04.2025
Scientific specialty code: 1.3.8

The impact of doping with rare earth elements, in particular with triple-charged lanthanides Ln^{3+} (Ln = Pr, Nd, Eu, Ce, Sm), on the luminescent properties of calcium tungstate featuring a scheelite structure produced by the microfluidic method was studied. The results of X-ray excited optical luminescence (XEOL) allow stating that doping with europium leads to the most intense luminescence of scheelite. A quantitative analysis of the elemental composition of scheelite samples obtained by the microfluidic method was carried out using the X-ray fluorescence analysis method, as well as a qualitative analysis of the X-ray absorption spectra (XANES) near absorption L_3-edge of W for Eu-substituted tungstate, as a sample providing the highest fluorescence yield.

Keywords: XEOL; scintillator; photodynamic therapy; XANES; microfluidics.

DOI: 10.51368/1996-0948-2025-2-84-89

Introduction

Photodynamic therapy (PDT) is the modern approach in cancer treatment which uses a photosensitiser which, when excited, usually in the optical range, is able to generate the reactive oxygen species (ROS) which, in turn, are able to locally cause the apoptosis of pathogenic cells and tissues where photosensitiser molecules are concentrated [1, 2]. The PDT mechanism can potentially be considered as an effective non-invasive method for treatment of deep-seated tumors, provided the systems can be excited using the penetrating ionizing radiation, for example, in the gamma or X-ray range. This version of the approach is known as the X-ray photodynamic therapy. However, although the first works on the application of X-ray radiation for exciting the photosensitiser and subsequent generation of ROS were published as long as a half a century ago [3], the current implementation of this technique on the widespread basis requires to develop biocompatible nanoparticles comprising heavy elements and featuring the highly efficient absorption of ionizing radiation and subsequent energy transfer to the

photosensitiser molecules [4]. When the highly efficient energy transfer is achieved, this mechanism can lead to local death of cancer cells even at low radiation load rates.

Introduction of rare earth elements (REE) such as lanthanides into the structure, which exhibit scintillation properties due to electronic transitions within f-orbitals [5, 6], allows creating more efficient X-ray phosphors, while variability of dopant types and concentrations allows shifting the emission spectrum density of phosphors [7], thereby allowing to use a larger number of photosensitizers. Calcium tungstate with a scheelite structure, which is widely used in medical imaging studies and may find application in theranostics, has a promising potential as a host lattice [8]. Modern synthesis methods, such as a microfluidic technique, allow producing more defective structures, including those with a distorted crystal lattice, without long-term heat treatment.

The findings of the optical and structural analysis of the calcium tungstate's defective structures obtained during the research, which can be used to form nanocomposites for X-ray photodynamic therapy, are provided herein.

Reagents

Doped scheelite was produced using sodium tungstate dihydrate $Na_2WO_4{\times}2H_2O$ (M.W.: 329.86 g/mol, 98 %, Sisco Research Laboratories Pvt. Ltd.), anhydrous calcium chloride $CaCl_2$ (M.W.: 110.98 g/mol, ≥93 %, Sigma-Aldrich), europium(III) chloride hexahydrate $EuCl_3{\times}6H_2O$ (M.W.: 446.07 g/mol, 99.99 %, REacton), neodymium(III) chloride hexahydrate $NdCl_3{\times}6H_2O$ (M.W.: 358.69 g/mol, 99.99 %, REacton), anhydrous samarium(III) chloride $SmCl_3$ (M.W.: 256.72 g/mol, 99.9 %, Alfa Aesar), cerium(III) chloride anhydrous $CeCl_3$ (M.W.: 246.48 g/mol, 99.5 %, Alfa Aesar), praseodymium(III) chloride hexahydrate $PrCl_3{\times}6H_2O$ (M.W.: 355.36 g/mol, 99.99 %, REacton).

Production procedure

To produce materials with the theoretical formula $Ca_{0,925}Ln_{0,05}WO_4$ ($Ln^{3+} = Pr^{3+}$, Nd^{3+}, Eu^{3+}, Ce^{3+}, Sm^{3+}) using the microfluidic method, two solutions were prepared: solution A contained 0.3 mol/L of sodium tungstate dihydrate, solution B contained 0.278 mol/L of anhydrous calcium chloride and 0.015 mol/L of lanthanide salt. The solutions were put in separate syringes and secured in high-precision pumps in the microfluidic platform. After that the flows of solutions A and B were mixed through a Y-shaped connector and the resulting mixture was fed through a polyethylene terephthalate (PET) tube with an internal diameter of 1.0 mm and a length of 1 m at different rates: the A:B rate ratio was either 1:1 or 1:4, as in [9]. The flow rates were set equaling to 5 µl/s for solution A and to 5 µl/s or 20 µl/s for solution B. The white precipitate formed during the reaction was collected in a separate collecting tube, precipitated by centrifuging at 10,000 rpm for 10 minutes, decanted, washed with bidistilled water three times, and dried at 60 °C.

Equipment

X-ray patterns were obtained by means of Bruker D2 Phaser desk-top X-ray diffractometer (Germany) at 30 kV, 10 mA Cu K_α radiation using a low-background cell. The range is 2θ – 10°–60°, the step is 0.01°. The elemental composition was analyzed using Bruker M4 TORNADO X-ray

microfluorometer (Germany). The obtained quantitative values of the elemental composition were averaged based on results of measurement at 20 points on the sample surface with measurement duration of 10 s per point. X-ray excited optical luminescence XEOL was measured using a special bench designed on the basis of commercial Cary Eclipse fluorimeter (Australia) and RAP90-5 X-ray tube and previously described in [10].

The emission slit width of the fluorimeter was 10 nm, and the exposure time was 0.1 s per point of the recorded XEOL signal. The operating parameters of the X-ray tube were 35 kV and 1.6 mA. X-ray absorption spectra in the XANES (X-ray absorption near edge structure) region were measured by the structural material engineering station of the Kurchatov synchrotron radiation source [11] using the silicon Si(311) monochromator for changing the energy of incident X-ray radiation on the sample.

Findings and discussion

According to the X-ray phase analysis data (Fig. 1), the samples produced by the microfluidic method are single-phase, and the X-ray pattern peaks correspond to the data of PDF-2 record with number 00-077-2236, $CaWO_4$ of the scheelite structure.

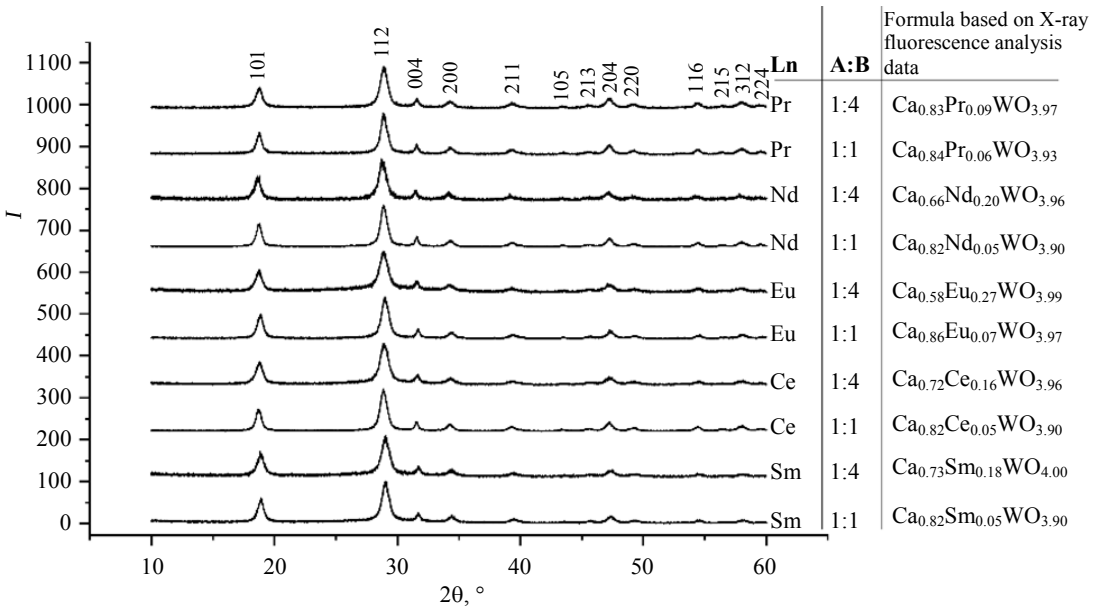

Fig. 1. X-ray patterns of $CaWO_4$:Ln samples where Ln = Pr, Nd, Eu, Ce, Sm, obtained by the microfluidic method with different ratios of flow rates: A ($Na_2WO_4 \times 2H_2O$) to B ($CaCl_2$/$LnCl_3$)

The elemental composition of the materials was determined using X-ray fluorescence analysis. The atomic percentage was recalculated based on the tungsten (W) content assumed to be equal to one. In this way, quantitative values of the content were obtained for calcium (Ca) and lanthanides (Pr, Nd, Eu, Ce, Sm). The quantitative content of oxygen atoms was calculated based on the electrical neutrality principle. The stoichiometric formulas of the samples under study are given in Fig. 1. A degree of calcium substitution by the Ln^{3+} cation has been found dependent on the ration of flow rates. As can

be seen from the findings of the quantitative elemental analysis, the degree of substitution varies between 5 % and 7 % at the similar flow rates for all dopants. But as the flow rate of mixture B increases up to 20 µl/s, the degree of substitution of Ca ions rare earth elements ions is seen to grow considerably, by 16–27 %, except for Pr, where the increase of flow B rate results in the degree of substitution of 9 %.

The samples containing Eu as a dopant were taken for XANES. These samples were prepared as powders and densely applied on the kapton. To calibrate the energy scale of the recorded X-ray absorption spectra, a reference sample – a tungsten oxide (WO_3) pellet placed between the second and third ionization chambers – was analyzed simultaneously. Normalization, calibration of the energy position and averaging of several measurement results were carried using DEMETER software [12].

Normalized XANES spectra obtained beyond L_3-edge of tungsten are shown in Fig. 2. The more intense absorption maximum observed in the $CaWO_4$:Eu sample can be explained by the higher density of free states on the d- or d-p-hybridized tungsten shells as compared to those in the tungsten-containing precursor. Peak *I* located at 10213 eV, is a "white line" corresponding to the oxidation state of tungsten +6. Peak *II* corresponds to the tetrahedron-shaped environment of tungsten for $CaWO_4$:Eu, and as for $Na_2WO_4{\times}2H_2O$ precursor, octahedral complexes are most likely to form due to the presence of crystalline water, which manifests itself in splitting of d-orbitals into two sublevels: *e_g* at 10230 eV and t_2g at 10220 eV. According to the XANES spectroscopy data, tungsten atoms in the obtained sample have a tetragonal coordination corresponding to the scheelite-type structure.

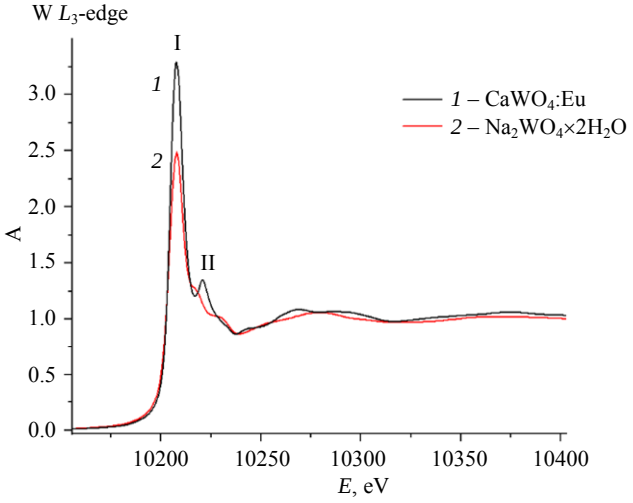

Fig. 2. XANES spectra beyond L_3-edge of tungsten for $CaWO_4$:Eu (A:B = 1:1) as compared to tungsten-containing precursor $Na_2WO_4{\times}2H_2O$, where A is normalized absorption

According to the literature data, pure calcium tungstate in the XEOL spectra exhibits a wide peak $^1T_2 \rightarrow {}^1A_1$ at 450 nm due to the Jahn-Teller effect, which affects the degenerated excited states of the tetrahedron WO_4^{2-} [13]. As shown in Fig. 3, doping with some lanthanides intensifies the initial luminescence of calcium tungstate and transfers the emission into the visible range, thus allowing to use a wide range of sensitizers. Adding Eu^{3+} and Nd^{3+} ions provides the maximum intensification of the initial scintillation of calcium tungstate around 450 nm, since $^1T_2$ energy levels of complex WO_4^{2-} resonate with the lanthanide transitions 4f→4f. Simultaneously, Sm^{3+} and Ce^{3+} ions effectively capture the excited state energy of the host matrix due to closely spaced energy levels, which leads to the nonradiative relaxation and quenching of luminescence. Whereas the high sensitivity of lanthanides' emission characteristics towards the crystalline environment of the host lattice as applied to praseodymium results in competition between the intrinsic luminescence of Pr^{3+} ions and WO_4^{2-} states due to nonresonant interaction [14].

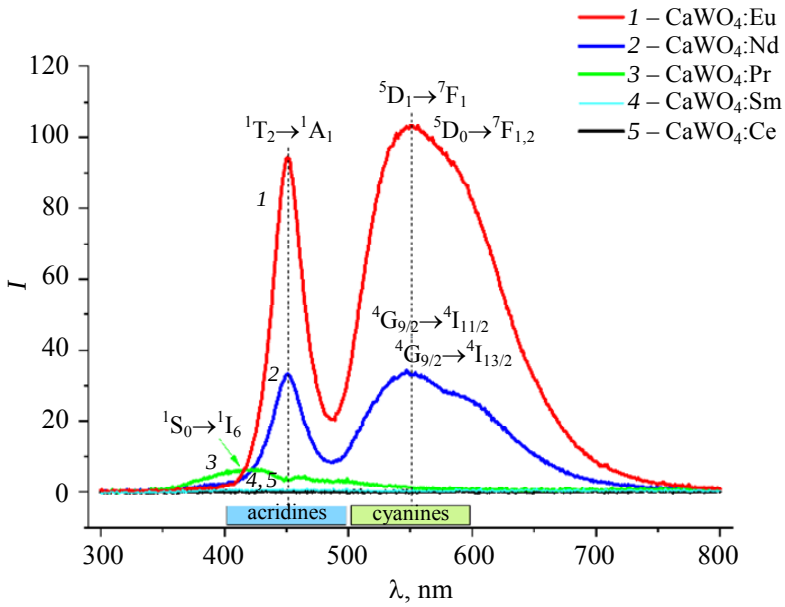

Fig. 3. Spectra of XEOL samples obtained at similar rates of flows A ($Na_2WO_4 \times 2H_2O$) and B ($CaCl_2/LnCl_3$)

Conclusion

- The microfluidic method is effective for low-temperature doping of scheelite using lanthanides.
- Four-fold increase of the rate of the flow containing doping elements results in the exponential growth of the Ca→Ln substitution percentage. The maximum substituent concentration amounted to 27% (for the Eu substituted sample).
- The most effective substitutes of calcium in scheelite, which contribute to a significant increase of the radiation intensity when irradiated in the X-ray range, are europium (+3) and neodymium (+3). Praseodymium (+3) exhibits the inherent luminescence, but suppresses the scintillation of the tungstate ion. Doping with samarium (+3) and cerium (+3) results in complete quenching of the X-ray luminescent properties.
- The obtained X-ray phosphors can be potentially used for X-ray PDT combined with photosensitizers of the acridine group (adsorption maximum of 400–500 nm) and cyanine group (adsorption maximum of 500–600 nm).

The study was carried out with financial support from the Ministry of Science and Higher Education of the Russian Federation within the framework of the state assignment in the field of scientific activity No. FENW-2023-0019.

REFERENCES

1. Diamond I., Mcdonagh A., Wilson C., Granelli S., Nielsen S. and Jaenicke R., Lancet **300** (7788), 1175–1177 (1972).
2. Dolmans D., Fukumura D. and Jain R., Nat. Rev. Cancer. **3** (5), 380–387 (2003).
3. Dougherty T. J., Grindey G. B., Fiel R., Weishaupt K. R. and Boyle D. G., JNCI **55** (1), 115–121 (1975).
4. Zhang T., Zheng H., Zhang F., Chu C., Liao T., Xie L., Liu G. and Cai W., J. Lumin **261**, 119862 (2023).
5. Maksimchuk P. O., Hubenko K. O., Bespalova I. I., Sorokin A. V., Borovoy I. A. and Yefimova S. L., J. Mol. Liq. **330**, 14–16 (2021).
6. Luo Z., Mao D., Li X., Luo J., Gong C. and Liu X., Coord. Chem. Rev. **508**, 215773 (2024).
7. Gu C., Wang Z., Pan Y., Zhu S. and Gu Z., Advanced Materials **35** (1), (2023).
8. Lei L., Wang Y., Kuzmin A., Hua Y., Zhao J., Xu S. and Prasad P. N., eLight **2** (1), 17 (2022).
9. Chen Z., Song Q., Ni L., Jiang J. and Yu Y., J. Environ. Chem. Eng. **9** (6), 106528 (2021).

10. Medvedev P. V., Pankin I. A., Soldatov M. A., Polozhentsev O. E. and Soldatov A. V., Opt. Spectrosc. **130** (6), 409–417 (2022).

11. Chernyshov A. A., Veligzhanin A. A. and Zubavichus Y. V., Nucl. Instrum. Methods Phys. Res. A **603** (1–2), 95–98 (2009).

12. Ko J. Y. P., Hu Y., Armelao L. and Sham T.-K., J. Phys. Conf. Ser. **190**, 012078 (2009).

13. Ravel B. and Newville M., J Synchrotron Radiat. **12** (4), 537–541 (2005).

14. Xiang Z., Jiang C., Liu C., Xie J. and Li H., eLight **2** (1), 6 (2022).

About authors

Polina Dmitrievna Kuznetsova, laboratory assistant, International Research Institute of Smart Materials of the Southern Federal University (344090, Russia, Rostov-on-Don, Andrey Sladkov St., 178/24). E-mail: pkuznecova@sfedu.ru SPIN code 9722-8406, Author ID 1288722

Elizaveta Andreevna Mukhanova, Head of the research laboratory, Candidate of Chemical Sciences, International Research Institute of Smart Materials of the Southern Federal University (344090, Russia, Rostov-on-Don, Andrey Sladkov St., 178/24). E-mail: kand@sfedu.ru SPIN code 4212-9848, Author ID 223100

Kirill Konstantinovich Volik, laboratory assistant, International Research Institute of Smart Materials of the Southern Federal University (344090, Russia, Rostov-on-Don, Andrey Sladkov St., 178/24). E-mail: kvolik@sfedu.ru SPIN code 2535-0515, Author ID 1288534

Ilya Andreevich Pankin, Head of the research laboratory, Candidate of Physics and Mathematics, International Research Institute of Smart Materials of the Southern Federal University (344090, Russia, Rostov-on-Don, Andrey Sladkov St., 178/24). E-mail: pankin@sfedu.ru SPIN code 3152-7393, Author ID 793405

Alexander Vladimirovich Soldatov, Head of the research group, Doctor of Physics and Mathematics, International Research Institute of Smart Materials of the Southern Federal University (344090, Russia, Rostov-on-Don, Andrey Sladkov St., 178/24). E-mail: soldatov@sfedu.ru SPIN code 2132-5994, Author ID 1685